Electronic Supplementary Information

Methyl camouflage in the ten-vertex *closo*-dicarbaborane(10) series. Isolation of *closo*-1,6-$R_2C_2B_8Me_8$ (R = H and Me) and their monosubstituted analogues

Mario Bakardjiev, Oleg L. Tok, Aleš Růžička, Zdeňka Růžičková, Josef Holub, Drahomír Hnyk, Zbyněk Špalt, Jindřich Fanfrlík, and Bohumil Štíbr*

Dalton Trans.

Key NMR measurements ($CDCl_3$)

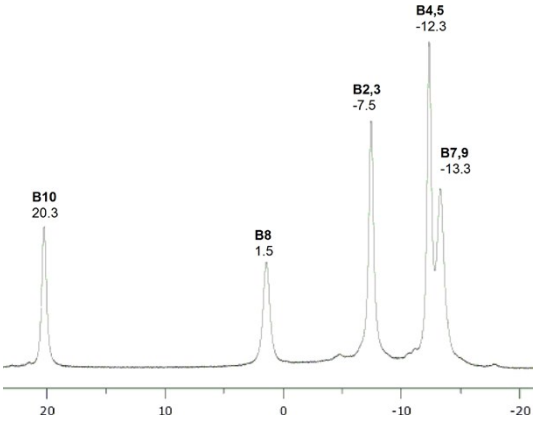

Figure S1. 190.2 MHz ^{11}B-NMR spectrum of 1,6-$H_2C_2B_8Me_7$-8-OTf (**2b**)

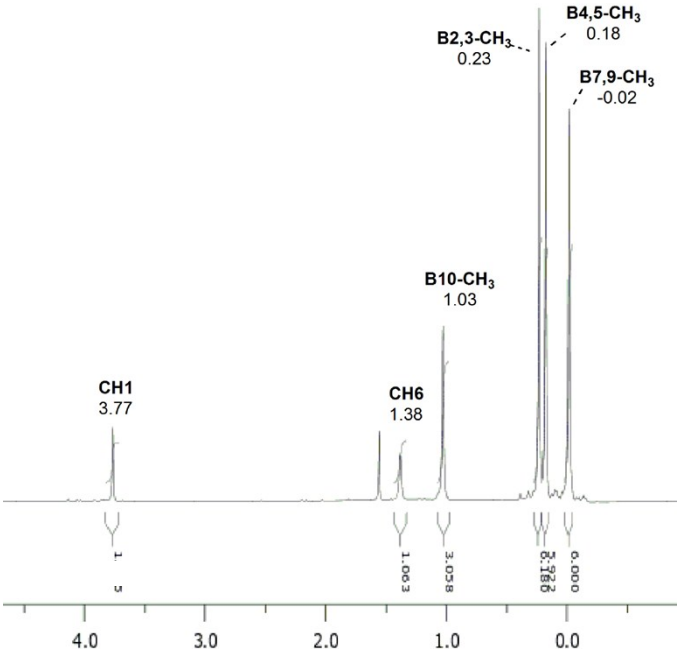

Figure S2. 600 MHz ^{1}H-NMR spectrum of 1,6-$H_2C_2B_8Me_7$-8-OTf (**2b**)

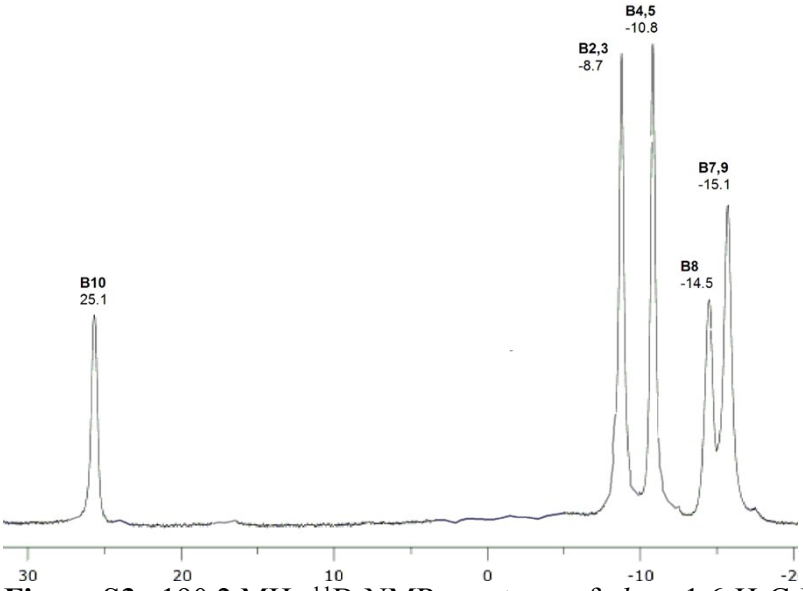

Figure S3. 190.2 MHz ^{11}B-NMR spectrum of *closo*-1,6-$H_2C_2B_8Me_7$-8-I (**2c**)

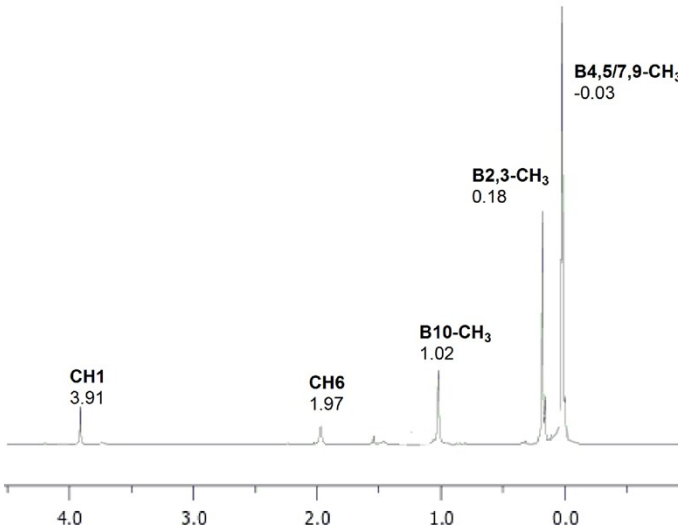

Figure S4. 600 MHz ^{1}H-NMR spectrum of *closo*-1,6-$H_2C_2B_8Me_7$-8-I (**2c**)

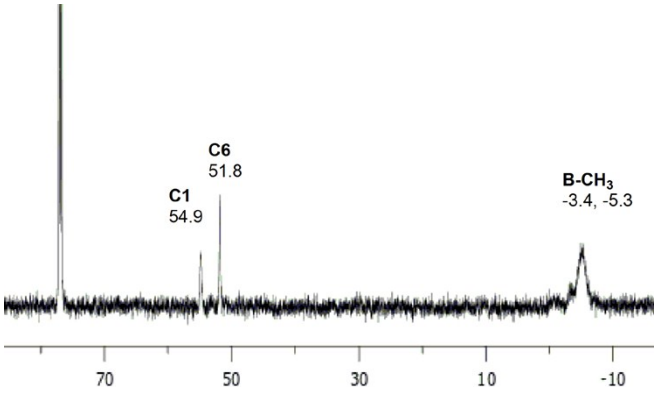

Figure S5. 150.9 MHz ^{13}C-NMR spectrum of *closo*-1,6-$H_2C_2B_8Me_7$-8-I (**2c**)

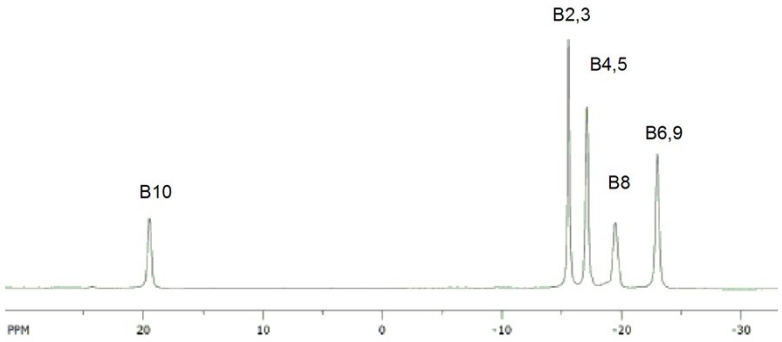

Figure S6. 190.2 MHz ^{11}B-{^{1}H}-NMR spectrum of 1,6-$Me_2C_2B_8H_8$ (**1b**)

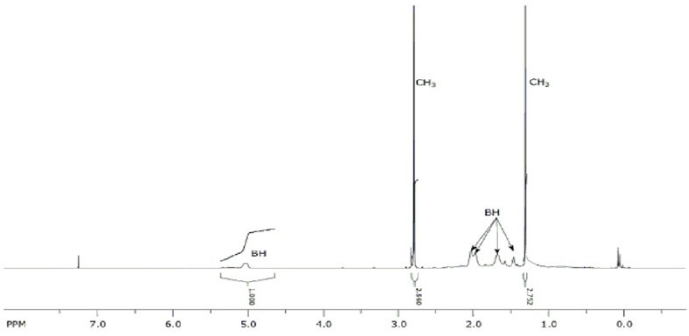

Figure S7. 600 MHz ^{1}H-{^{11}B} NMR spectrum of 1,6-$Me_2C_2B_8H_8$ (**1b**)

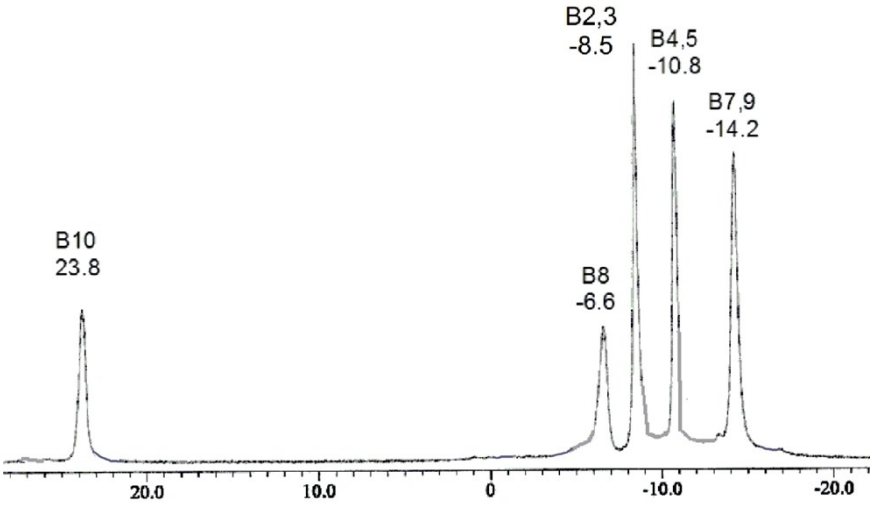

Figure S8. 190.2 MHz ^{11}B NMR spectrum of *closo*-1,6-$Me_2C_2B_8Me_8$ (**4a**)

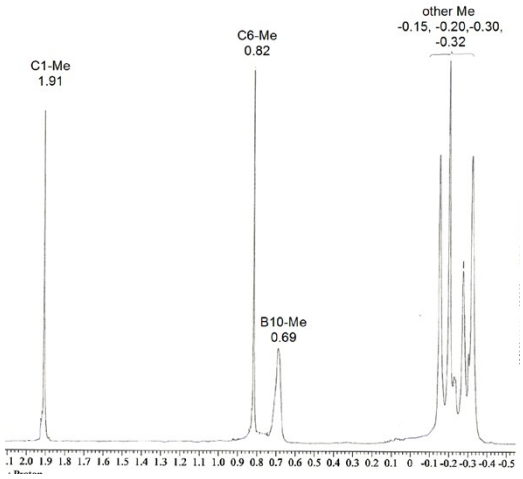

Figure S9. 600 MHz ^{1}H NMR spectrum of *closo*-1,6-$Me_2C_2B_8Me_8$ (**4a**)

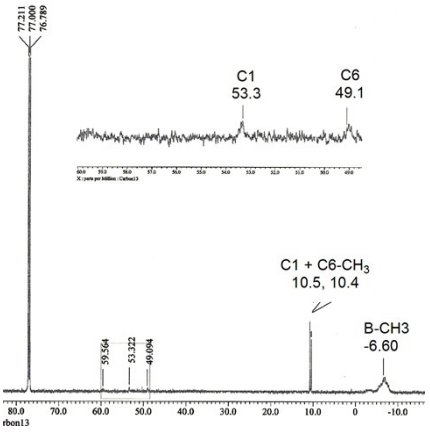

Figure S10. 150.9 MHz ^{13}C NMR spectrum of *closo*-1,6-$Me_2C_2B_8Me_8$ (**4a**)

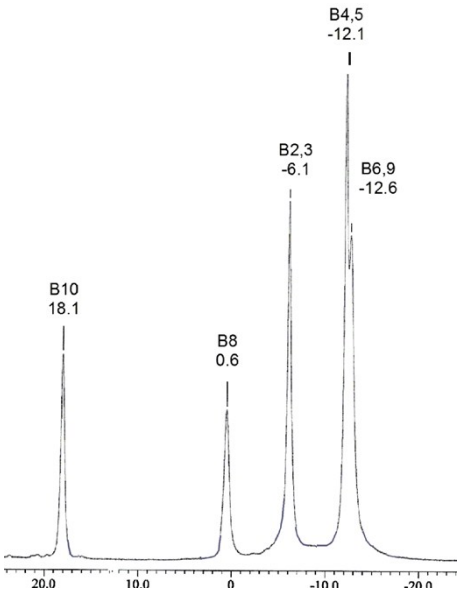

Figure S11. 190.2 MHz ^{11}B NMR spectrum of *closo*-1,6-$Me_2C_2B_8Me_7$-8-OTf (**4b**)

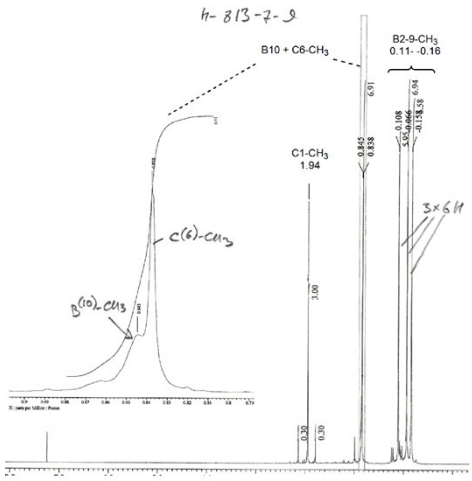

Figure S13. 600 MHz ^{1}H NMR spectrum of *closo*-1,6-$Me_2C_2B_8Me_7$-8-OTf (**4b**)

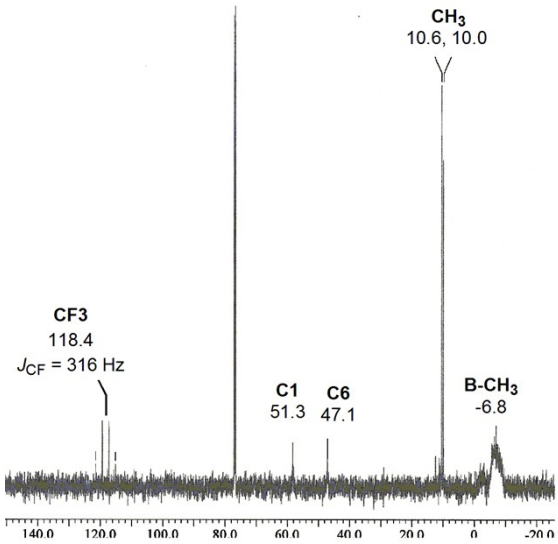

Figure S14. 150.9 MHz ^{13}C NMR spectrum of *closo*-1,6-$Me_2C_2B_8Me_7$-8-OTf (**4b**)

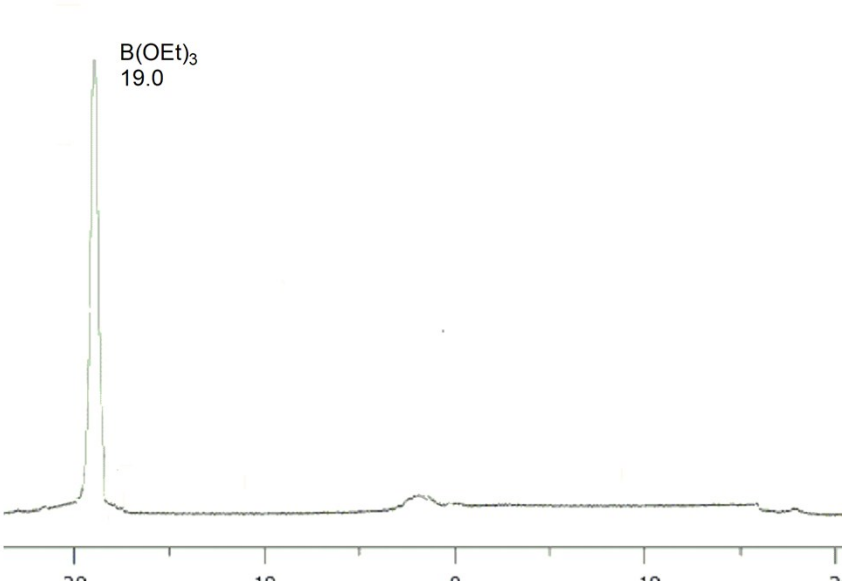

Figure S15. 128.3 MHz ^{11}B NMR spectrum of *closo*-1,6-$H_2C_2B_8H_8$ (**1a**) after a 10 h-exposure to EtOH. The spectrum of *closo*-1,6-$H_2C_2B_8Me_8$ (**2a**) has not changed (see Figs. 5 and S15) after 48 h under similar conditions.

Comparative NMR stick diagrams

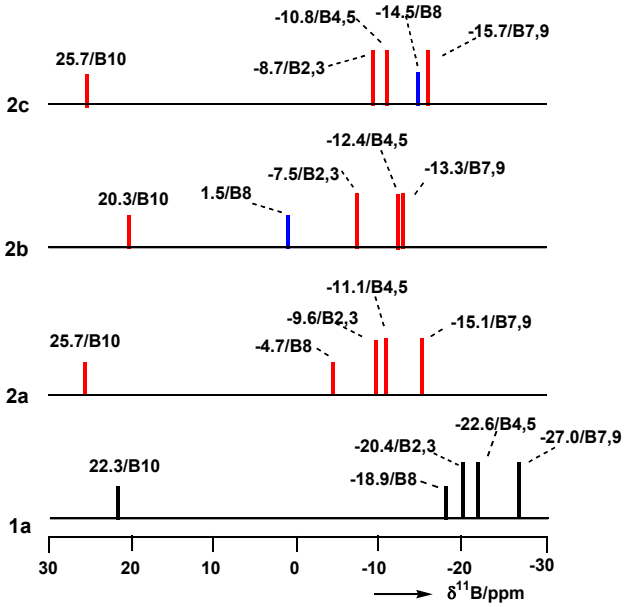

Figure S15. Stick diagrams comparing the ^{11}B NMR chemical shifts (128 or 190 MHz) and relative intensities for *closo* compounds 1,6-$H_2C_2B_8H_8$ (**1a**),[6] 1,6-$H_2C_2B_8Me_8$ (**2a**), 1,6-$H_2C_2B_8Me_7$-8-OTf (**2b**), and 1,6-$H_2C_2B_8Me_7$-8-I (**2c**). Red sticks indicate the B-Me singlets, blue the B-X signals; black sticks stand for BH doublets.

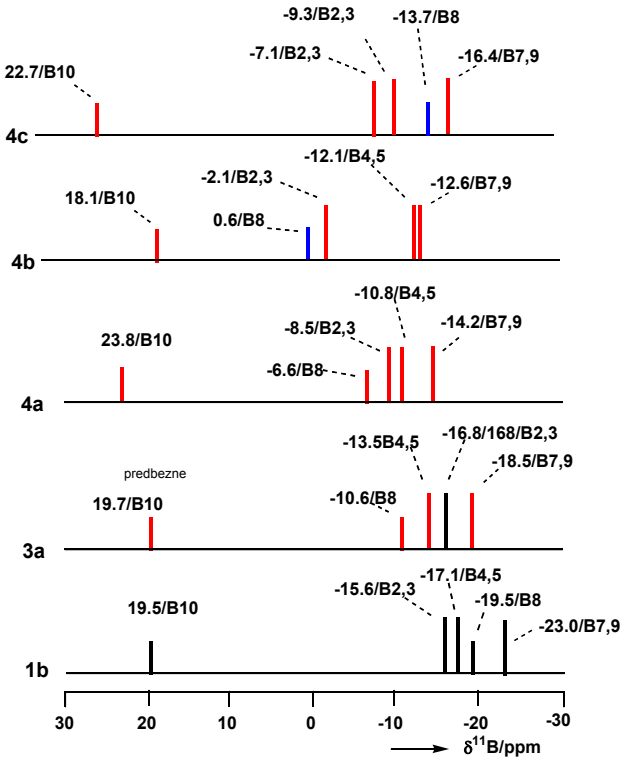

Figure S16. Stick diagrams comparing the ^{11}B NMR chemical shifts (128.3 or 190.2 MHz) and relative intensities for *closo* compounds 1,6-$Me_2C_2B_8H_8$ (**1b**), 1,6-$Me_2C_2B_8Me_8$ (**4a**), 1,6-$Me_2C_2B_8Me_7$-8-OTf (**4b**), and 1,6-$Me_2C_2B_8Me_7$-8-I (**4c**). Red sticks indicate the B-Me singlets, blue the B-X signals; black sticks stand for BH doublets.

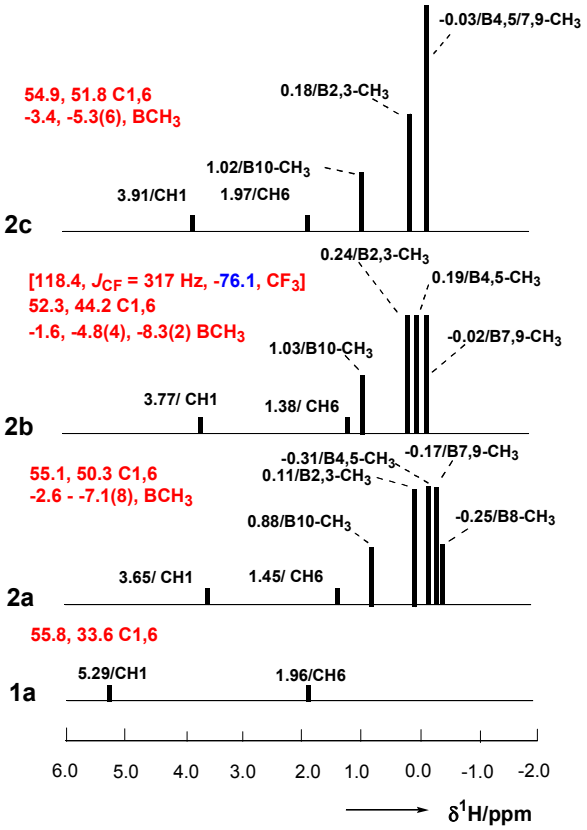

Figure S17. Stick diagrams comparing the ^{1}H (black sticks), ^{13}C (red text), and ^{19}F (blue text) NMR chemical shifts and relative intensities for *closo* compounds 1,6-$H_2C_2B_8H_8$ (**1a**), 1,6-$H_2C_2B_8Me_8$ (**2a**), 1,6-$H_2C_2B_8Me_7$-8-OTf (**2b**), and 1,6-$H_2C_2B_8Me_7$-8-I (**2c**).

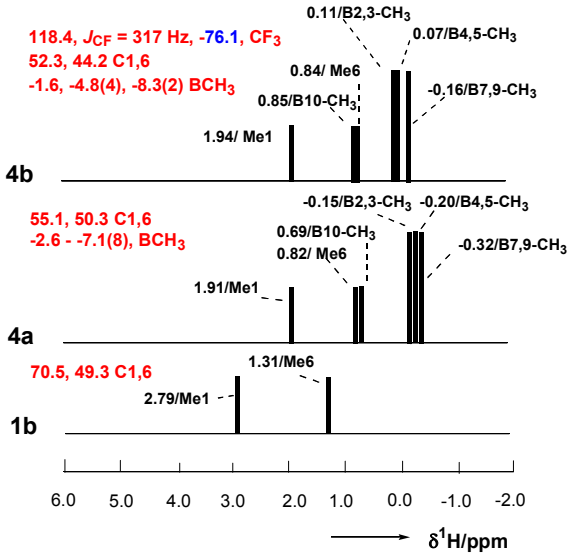

Figure S18. Stick diagrams comparing the ^{1}H (black sticks), ^{13}C (red text), and ^{19}F (blue text) NMR chemical shifts and relative intensities for *closo* compounds 1,6-$Me_2C_2B_8H_8$(**1b**), 1,6-$Me_2C_2B_8Me_8$ (**4a**) and 1,6-$H_2C_2B_8Me_7$-8-OTf (**4b**).

Geometry optimization

Cartesian geometry for 2a (MP2/TZVP)

	x	*y*	*z*
C	-0.01756	-1.71037	0.60349
B	-0.95469	-1.2324	-0.59318
B	0.93407	-1.24687	-0.58701
B	0.91692	-0.49508	1.09623
B	-0.93709	-0.48227	1.08962
C	0.00101	-0.03153	-1.40529
B	1.31467	0.49596	-0.35221
B	0.00382	1.06734	0.8134
B	-1.31096	0.51645	-0.35892
B	0.01101	1.48686	-0.833
H	-0.02594	-2.70395	1.02847
C	-1.94255	-2.17563	-1.37837
C	1.91253	-2.20587	-1.36487
C	-1.97074	-0.63312	2.27773
C	1.94087	-0.66397	2.29053
H	0.00229	-0.11839	-2.48932
C	-2.76361	1.00387	-0.78159
C	2.77684	0.96187	-0.76568
C	0.03324	2.18814	1.94262
C	0.0189	2.8284	-1.65349
H	-2.54133	0.28361	2.44053
H	-2.68564	-1.4378	2.08251
H	-1.45966	-0.8736	3.21455
H	-2.47955	-1.64488	-2.16661
H	-1.41318	-3.0156	-1.83678
H	-2.68851	-2.59565	-0.69815
H	2.46332	-1.68447	-2.14977
H	2.64693	-2.63671	-0.67887
H	1.37337	-3.03794	-1.82626
H	2.53865	0.23639	2.44612
H	1.41811	-0.8766	3.22764
H	2.63155	-1.49261	2.1089
H	3.55675	0.2981	-0.38566
H	2.87544	0.99821	-1.85475
H	-0.06923	3.69093	-0.98801
H	0.94421	2.95094	-2.22274
H	-0.81401	2.87655	-2.36002
H	-2.84531	1.07708	-1.87015
H	-3.55439	0.33475	-0.43491
H	-2.96779	2.00101	-0.38257
H	-0.53858	3.07454	1.65481
H	-0.35933	1.8356	2.89973
H	1.06215	2.51768	2.11924
H	2.9829	1.96998	-0.39646

Cartesian geometry for 4a (MP2/TZVP)

	x	*y*	*z*
C	-1.67976	0.01277	-0.09657
B	-0.68902	1.10738	-0.7116
B	-0.67946	-0.73962	-1.09388
B	-0.81289	-1.09746	0.7036
B	-0.82447	0.71501	1.08218
C	0.77795	0.23167	-1.0913
B	0.7492	-1.31189	-0.1678
B	0.69222	-0.28224	1.3713
B	0.73437	1.27691	0.37223
B	1.81803	-0.01751	0.13253
C	-3.18727	0.04239	-0.22991
C	-1.20609	2.30121	-1.6192
C	-1.18426	-1.47834	-2.40361
C	-1.55703	1.51842	2.24503
C	-1.53874	-2.30662	1.44182
C	1.40793	0.51797	-2.4493
C	1.35656	2.73788	0.55266
C	1.38583	-2.71922	-0.578
C	1.17837	-0.598	2.86322
C	3.39987	0.01121	0.05853
H	-3.4998	-0.1312	-1.26504
H	-3.65352	-0.72846	0.39194
H	-3.59367	1.01011	0.08196
H	-0.85	1.9777	2.94458
H	-2.18745	2.32654	1.85048
H	-2.21287	0.86413	2.83396
H	-0.40216	2.96756	-1.94959
H	-1.72361	1.93996	-2.51751
H	-1.92805	2.91822	-1.06913
H	-0.37019	-1.93729	-2.97456
H	-1.88817	-2.28037	-2.14812
H	-1.71651	-0.79752	-3.08132
H	-0.82825	-2.99761	1.90864
H	-2.20726	-1.95121	2.2371
H	-2.15362	-2.89805	0.75036
H	2.04241	-0.31983	-2.75709
H	0.66483	0.68608	-3.23401
H	2.04712	1.40517	-2.39124
H	1.85767	-3.18366	0.29742
H	0.65591	-3.43573	-0.97142
H	2.17862	-2.61413	-1.32969
H	3.84058	-0.14097	1.05146
H	3.80405	-0.77589	-0.591
H	3.78525	0.96845	-0.31594
H	2.13887	2.94875	-0.1878
H	0.61732	3.54406	0.48465
H	1.83832	2.82041	1.53534

H	2.2498	-0.41511	3.00947
H	0.64375	0.00166	3.61063
H	0.99831	-1.64878	3.12688

Computed δ(^{11}B) NMR chem. shifts (GIAO-MP2/II//MP2/TZVP) (in ppm, referenced to $BF_3.OEt_2$)

	B(2,3)	B(4,5)	B(7,9)	B(8)	B(10)
1a	-19.5	-21.0	-27.0	-18.4	22.5
2a	-7.2	-8.2	-13.8	-4.4	28.0
4a	-5.4	-7.9	-11.6	-4.2	26.0